Dynamic behavior of three-hinge type precast arch culverts installed in embankment with asymmetrical overburden in culvert longitudinal direction

AUTHOR(S):

Miyazaki, Y.; Sawamura, Y.; Kishida, K.; Kimura, M.

CITATION:

Miyazaki, Y. ...[et al]. Dynamic behavior of three-hinge type precast arch culverts installed in embankment with asymmetrical overburden in culvert longitudinal direction. Proceedings. of the 9th International Conference on Physical Modelling in Geotechnics 2018 2018: 915-920

ISSUE DATE:

2018-10-24

URL:

http://hdl.handle.net/2433/235499

Dynamic behavior of three-hinge-type precast arch culverts with various patterns of overburden in culvert longitudinal direction

Y. Miyazaki, Y. Sawamura, K. Kishida & M. Kimura

Kyoto University, Kyoto, Japan

ABSTRACT: Many three-hinge-type precast arch culverts suffered damage in the Great East Japan Earthquake (11 March 2011), which highlighted the importance of the elucidation of their seismic behavior. The degree of damage to the culverts appeared to be closely related to the seismic wave motions in the culvert longitudinal direction. Particularly severe damage, such as mouth wall deformation and damage to arch members, seems to have been caused mainly by asymmetrical embankment loading in the culvert longitudinal direction. Thus, in order to clarify the mechanisms behind these seismic damage patterns, centrifuge tests on model culverts with three-hinge-type construction and various embankment shapes were conducted here, and the behavior in the longitudinal direction was observed. As a result, it was clarified that the response acceleration of culverts located near a mouth wall with shallow embankment cover gets amplified and exceeds that of the surrounding embankment due to the decreased constraining effect of the embankment overburden.

1 INTRODUCTION

Hinge-type precast arch culverts (Figure 1) enable labor saving and high-quality control construction by using precast concrete arch members. According to the position of the hinge, hinge-type precast arch culverts are classified as the two-hinge type or the three-hinge type, although both types are stabilized by allowing a certain degree of movement to mobilize the passive resistance of the embankment.

In Japan, where earthquakes occur frequently, the seismic performance of precast arch culverts is closely related to the stability of the hinge, which may cause the collapse of the arch structures themselves. Therefore, the seismic behavior in the culvert transverse direction has been investigated (e.g., Toyota and Takagai, 2000) and identified as a critical issue in the section design of arch culverts. Sawamura et al. (2016a, b) conducted large shaking table tests in the culvert transverse direction (Figure 1) on one-fifth scale models of three-hinge-type precast arch culverts, evaluating the damage morphology and ultimate state, and observed no hinge slippage before the ultimate state of the RC arch member.

On the other hand, although most damage to road embankments is correlated with ground motions in the culvert longitudinal direction (Tokida et al., 2007), research literature remains insufficient (Miyazaki et al., 2016). In the Great East Japan Earthquake (11 March 2011), the resulting damage to precast culverts appears to have been caused by strong inertial forces in the longitudinal direction (Abe and Nakamura, 2014). Particularly in the old type of three-hinge arch culverts (Figure 2), severe damage occurred, such as deformation of the mouth wall, numerous cracks in the arch members, and patterned chipping of the foundation, as shown in Figure 3. These damaged culverts had one point in common, namely, they had either shallow soil cover or an asymmetrical embankment load in the culvert longitudinal direction due to the embankment slope.

Therefore, the aim of this study is to clarify the influence of embankment shape patterns on the seismic behavior and soil-structure interaction in the culvert longitudinal direction. Dynamic centrifuge tests on model three-hinge-type arch culverts were carried out for varied embankment geometries.

2 DYNAMIC CENTRIFUGE MODEL TESTS

2.1 *Experimental outline*

Centrifuge shaking table tests were conducted under a gravitational acceleration of 50 G using the geotechnical centrifuge device at Kyoto University's Disaster Prevention Research Institute (DPRI). A soil

chamber, 340 mm (H) ×450 mm (W) × 300 mm (D), was employed. Figures 4 and 5 show schematic drawings of the model embankments including arch culverts. Three-hinge-type arch culverts were modeled with a length of 28.8 m and constructed on a 5-m-deep layer of soil. In the experiment, a half-length section, 14.4 m in length, was modeled due to the limited dimensions of the soil chamber. The measurement items were as follows: horizontal acceleration of the ground, culvert and wall, horizontal displacement of the wall, and earth pressure acting on the wall. Tests were conducted for four cases, each having a different embankment shape, as depicted in Figures 4 and 5. The experimental parameters were the soil cover thickness and the distance between the mouth and the embankment toe. All other factors were kept constant. Due to concerns of the boundary condition of the back of the embankment, a 2-mm-wide gel sheet (compressive stress of 10% is 0.07 N/mm^2) was applied after the preliminary experiment using a rigid chamber. The gel sheet was set on the side wall of the chamber in the vertical direction against the shaking direction in order to decrease the influence of the reflected wave.

2.2 *Three-hinge-type arch model*

Figure 6 shows a schematic drawing of the three-hinge-type arch culvert model. The arch culvert model was designed based on the modern type (Figure 3), which has an invert foundation. The arch model member was made of aluminum and its thickness was adjusted to match the bending stiffness of a real RC member. Each arch member was arranged in a staggered distribution as in the actual construction method. The structural connection of the arch culverts was modeled by masking tape instead of the crown beam (Figure 3). The joints of each arch culvert were covered with polypropylene sheets to prevent the intrusion of sand.

2.3 *Mouth wall model*

Generally, mouth walls of three-hinge-type arch culverts are constructed as perpendicular reinforced soil walls. The wall structure is different near the mouth versus the rest of the reinforced soil wall (Figure 1). The wall near the culvert mouth is composed of two large concrete panels, which are joined by grouting. The other part of the wall is constructed as a typical reinforced earth wall. The wall in this experiment represents only the integrated wall near the culvert. Figure 7 shows the mouth wall model. A 5-mm-thick acryl panel was used for the wall model. Alu- minum plates, 0.1 mm in thickness and 10 mm in width, were employed for the reinforcing members. The foundation for the wall model was made of an aluminum angle plate with a thickness of 1 mm and a depth of embedment of 0.5 m in the prototype scale.

2.4 *Model ground and input wave*

Hinge-type arch culverts must be built to specific standards and applied to both embankment and foundation soils. Therefore, the model ground here was made by compacting wet Edosaki sand to Dc = 92% and w = 17.8% (= w_{opt} of Edosaki sand).

The wave was input by shaking in steps to focus on the changes in the displacement of the mouth wall and the response acceleration. A continuous tapered 1-Hz wave with 20 cycles of sine waves was applied. It was applied 10 times, from STEP 1 to 10, with a gradual increase of 0.5 m/s^2 per step. Figure 8 shows the input wave of STEP 5 as an example.

3 SEISMIC RESPONSE DUE TO ASYMMETRICAL OVERBURDEN IN CULVERT LONGITUDINAL DIRECTION

3.1 *Deflection mode of mouth wall*

In Figure 9, the transition of the wall turnover rate, the translation, and the migration area are plotted over all the excitation steps. The definition of each physical quantity is as follows. The turnover rate is the value of the difference ($\Delta_d = \Delta_1 - \Delta_2$) between the lateral displacements of the upper portion (Δ_1) and the lower portion (Δ_2) divided by the wall height (H). The translation is equal to Δ_2. The migration area is the product of the lateral displacement at the center of the wall ($\Delta_m = (\Delta_1 + \Delta_2) / 2$)) and the wall height ($H$). The figure shows the following relations:

Turnover rate: Case-4 > Case-3 > Case-2 > Case-1
Translation: Case-3 > Case-4 ≒ Case-2 > Case-1
Migration area: Case-4 > Case-3 > Case-2 >Case-1

The migration area is the path area of the wall model during excitation, which can be considered as an expression of the amount of embankment deformation. The length of the reinforcing members is constant across all experimental cases, which may result in decreased deformation in Case-4. However, the migration area increased proportionally to the gross weight of the embankment model.

3.2 *Seismic response of culverts and ground*

Figure 10 shows the transition of the maximum response acceleration at A_3, A_{Ring3}, and A_{Ring11} over all excitation steps. The maximum response acceleration is given by the average of the negative and positive peak values from t = 10.00 ~ 20.00 s. In Figure 10, the maximum acceleration in the left and right directions is plotted. According to the figure, the amplification of the response acceleration and the difference between A_{Ring3} and A_{Ring11} decreased more for cases with greater embankment cover. This is because an increase in soil cover strengthens the confining pressure acting on the culverts, which reduces the amplification of the response acceleration. On the other hand, in Case-1, the response acceleration of A_{Ring3} exceeded that of A_{Ring11} as well as that of A_3 at STEPS 8, 9, and 10.

As is shown in Figure 10, the acceleration relation among A_3, A_{Ring3}, and A_{Ring11} changed at STEP 8. To explain this relation, the hysteresis curve of the response acceleration is depicted in Figure 11 from t = 13.50 to 14.48 s. In the figure, the start and end points of the hysteresis curves are plotted.

The mutual relationship among A_3, A_{Ring3}, and A_{Ring11} in each experimental case is visible at peak response acceleration No. 3, at which the leftwards response acceleration is maximum. In Case-1, the response acceleration of A_{Ring3} exceeded that of A_{Ring11}. On the other hand, in Case-2 and Case-3, the response acceleration of A_{Ring3} was less than that of A_{Ring11}, and the difference between A_{Ring3} and A_{Ring11} was small. Compared with the curve shape of Case-1, the curve shapes of A_3, A_{Ring3}, and A_{Ring11} converge in Case-2 and Case-3. Moreover, the curve shapes of A_3, A_{Ring3}, and A_{Ring11} are almost coincident with each other in Case-4.

From the above results, the following can be concluded. In Case-1, where the overburden thickness is a constant 1.0 m in the culvert longitudinal direction, the seismic response exceeds that of the surrounding ground, and the highest amplification is observed at the mouth. In Case-2 and Case-3, a difference in acceleration values is seen between Ring 3 and Ring 11, but the difference decreases with increasing soil cover for the culverts. On the other hand, in Case-4, where the overburden thickness is a constant 4.0 m in the longitudinal direction, integrated behavior of the culverts and the surrounding ground is shown due to the large confining stress.

3.3 *Embankment model after excitation*

Figure 12 shows the embankment model surface after excitation with marked lines on the cracked areas. As seen in the figure, longitudinal cracks were observed in Case-1 ~ Case-3 near the small soil cover area at the mouth. The cracks run along the arch crown and seem to have been caused by tensile forces in the culvert transverse direction. The compressive deformation on the sides of the culverts is thought to have created tensile force on the ground surface in the crown area. On the other hand, in Case-4, large cracks occurred in the culvert transverse direction in the central area of the embankment surface. This is because large deformation of the mouth wall caused tension on the surface of the embankment. While the enlargement of the earth cover has the advantage of restraining the seismic behavior of culverts in the longitudinal direction, the larger transverse deformation of the embankment surface should be considered.

Figure 13 shows the mouth of the culverts after excitation. In this experiment, the hinge was designed as a simply butted section. That is why this hinge model would collapse more easily than an actual knuckle hinge. However, as seen in the figures, even when the embankment has large deformation, no slippage of the crown hinge is observed.

4 CONCLUSIONS

In this study, dynamic centrifuge model tests were conducted focusing on the influence of the embankment shape on the seismic performance of three-hinge arch culverts in the longitudinal direction. The following conclusions can be drawn from the results of this study:

1) The deformation of an embankment in the culvert longitudinal direction increases proportionally to the gross weight of the soil.
2) The seismic behavior of culverts in the longitudinal direction is closely related to the degree of overburden.

3) Shallow soil cover, such as 1.0 m, allows the response acceleration of culverts to be amplified and to exceed that of the surrounding soil at the mouth. Conversely, deep soil cover, of more than 4.0 m, causes the culverts to respond as an integrated body with the surrounding soil.
4) In the experiment in which the entire overburden was more than 1.0 m and in which the hinge was a simply butted section, no slippage of the hinge portion was observed during repeated excitation in the longitudinal direction.

ACKNOWLEDGEMENT

This work was supported by the RESEARCH FOUNDATION ON DISASTER PREVENTION OF EXPRESS HIGHWAY BY NEXCO-AFFILIATED COMPANIES.

REFERENCES

Abe, T. and Nakamura, M. 2014. *The use of and the caution in the application of the culvert constructed by large precast element in the expressway construction*, The Foundation Engineering & Equipment, Vol. 42, No. 4, pp. 8-11. (in Japanese)
Miyazaki, Y., Sawamura, Y., Kishida, K. and Kimura, M. 2017. Evaluation of dynamic behavior of embankment with precast arch culverts considering connecting condition of culverts in culvert longitudinal direction, Japanese Geotechnical Society Special Publication, Vol. 5, No. 2, pp. 95-100. http://doi.org/10.3208/jgssp.v05.020
Sawamura, Y., Ishihara, H., Kishida, K., and Kimura, M. 2016a. Experimental Study on Damage Morphology and Critical State of Three-hinge Precast Arch Culvert through Shaking Table Tests, Procedia Engineering, Advances in Transportation Geotechnics III, Vol. 143, pp. 522-529, 2016. http://dx.doi.org/10.1016/j.proeng.2016.06.066
Sawamura, Y., Ishihara, H., Kishida, K., and Kimura, M. 2016b. Evaluation of Damage Morphology in Three-Hinge Precast Arch Culvert Based on Shaking Table Tests and Numerical Analyses, Proc. of the 8th Young Geotechnical Engineering Conference, pp. 221-226, Astana, Kazakhstan.
Tokida, K., Oda, K., Nabeshima, Y. and Egawa, Y. 2007. Damage level of road infrastructure and road traffic performance in the mid Niigata prefecture earthquake of 2004, Structural Engineering/Earthquake Engineering, Vol. 24, No. 1, pp. 51-61.
Toyota, H. and Itoh, T. 2000. Effects of Shaking Conditions and Material Properties on Dynamic Behavior of Terre Armee Foundation and 3-Hinge Arch, Proc. of Japan Society of Civil Engineers, No. 666/III-53, pp. 279-289. (in Japanese)

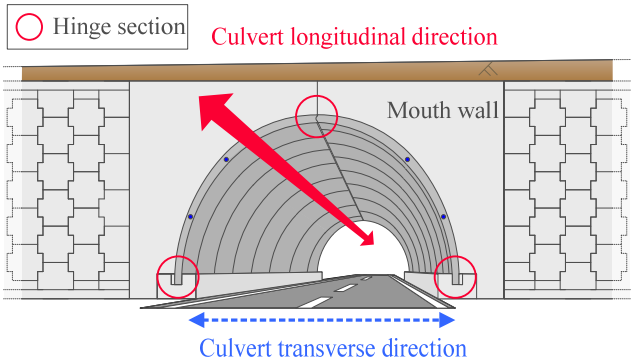

Figure 1. Three-hinge-type precast arch culverts installed in embankment

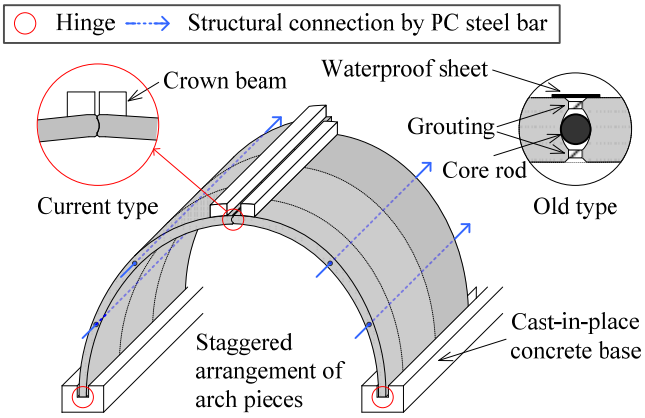

Figure 2. Schematic view of three-hinge arch culvert

Damaged foundation　　Deformation of mouth wall

Figure 3. Disaster examples from Great East Japan Earthquake (11 March 2011)

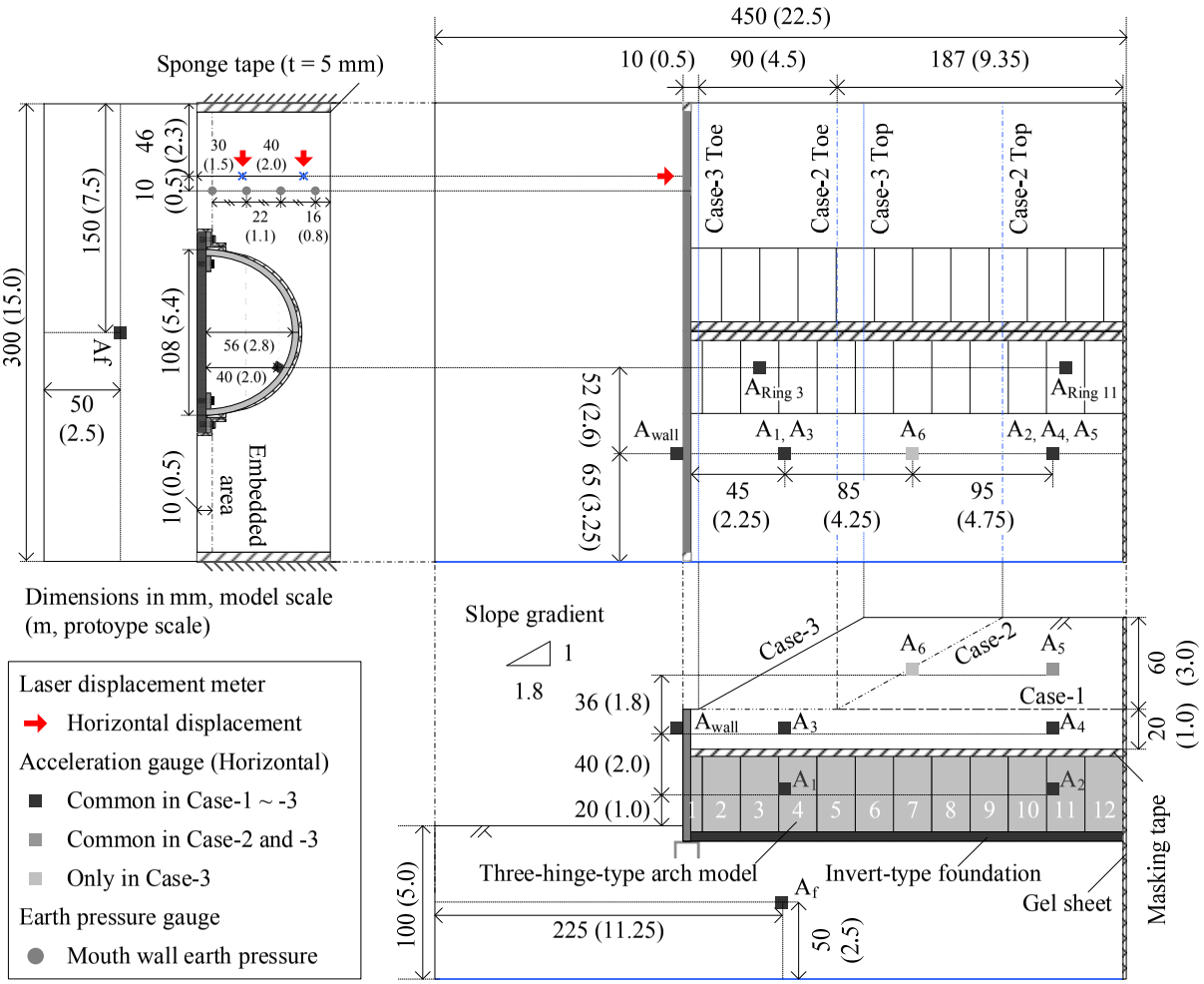

Figure 4. Experimental set-up in Case-1 ~ Case-3

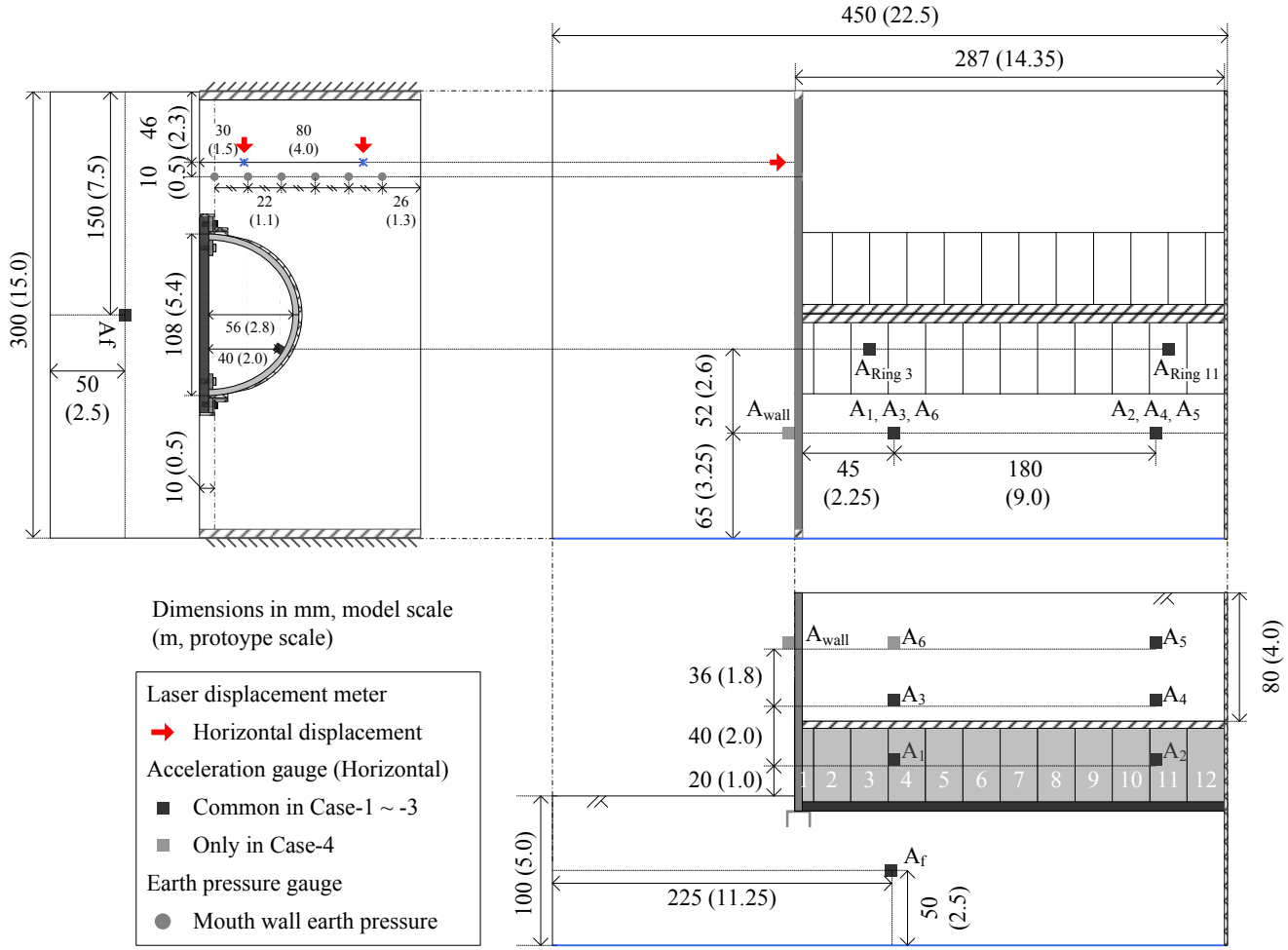

Figure 5. Experimental set-up in Case-4

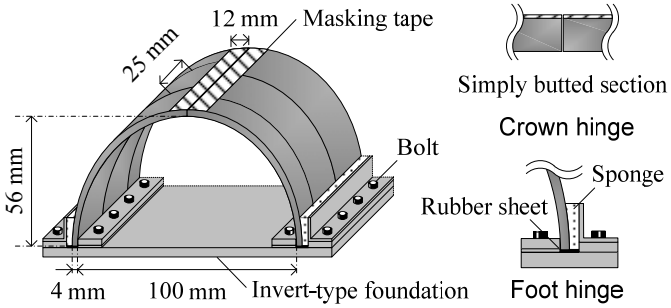

Dimensions in mm, model scale

Figure 6. Three-hinge arch culvert model

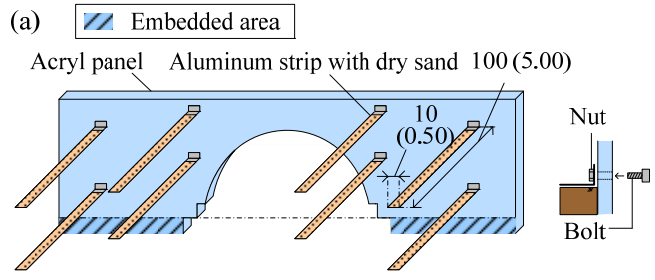

Dimensions in mm, model scale (m, protoype scale)

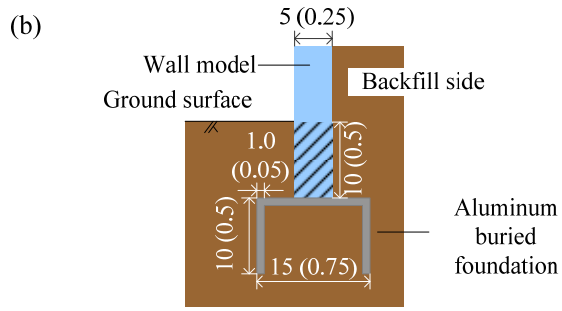

Dimensions in mm, model scale (m, protoype scale)

Figure 7. Schematic view of mouth wall model: (a) Structure of mouth wall model and (b) Structure of embedded area

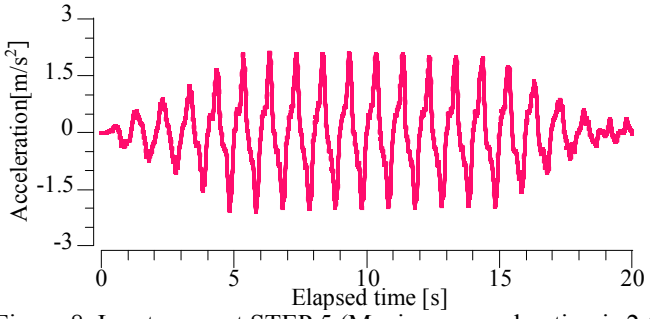

Figure 8. Input wave at STEP 5 (Maximum acceleration is 2.5 m/s^2)

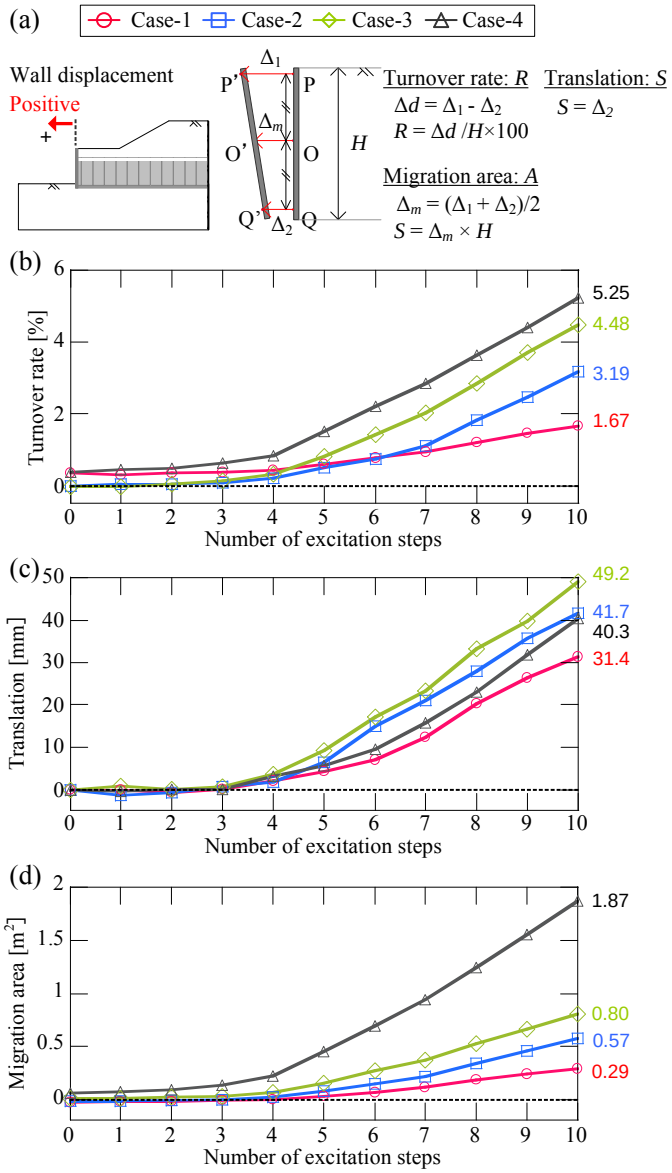

Figure 9. Deflection mode of mouth wall model: (a) Definition of physical quantity, (b) Transition of turnover rate, (c) Transition of translation, and (d) Transition of migration area

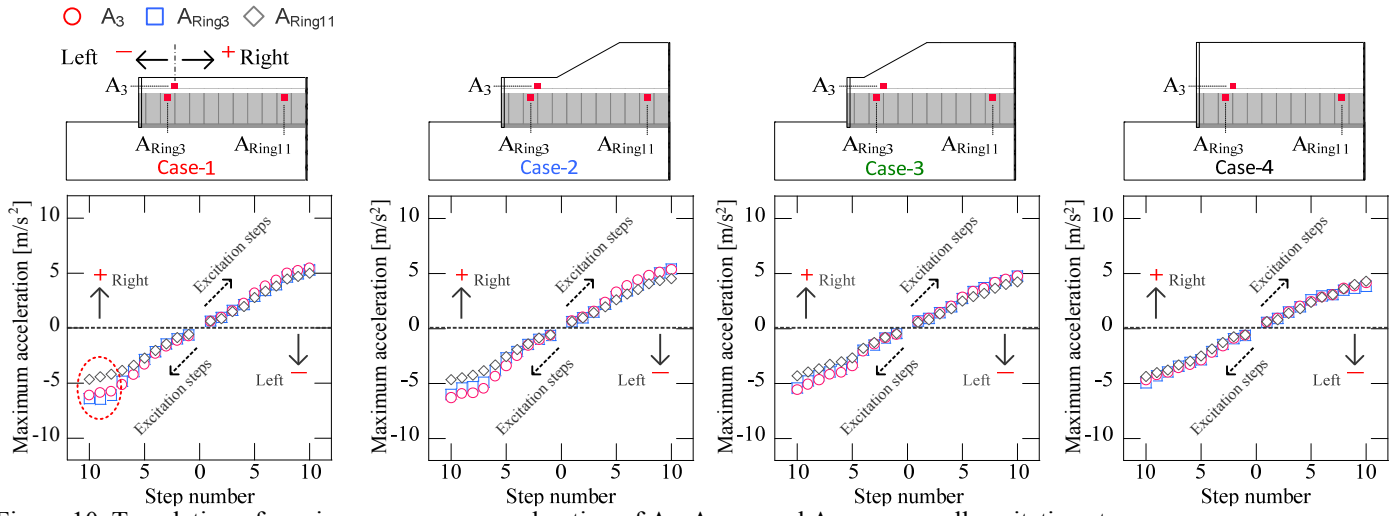

Figure 10. Translation of maximum response acceleration of A_3, A_{Ring3}, and A_{Ring11} over all excitation steps

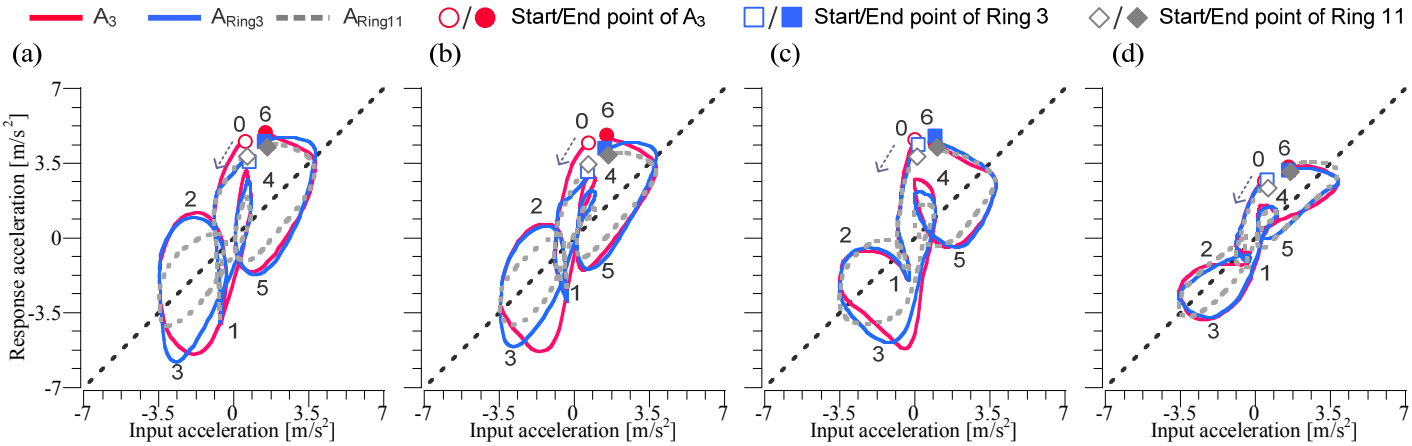

Figure 11. Hysteresis curves of response acceleration of A_3, A_{Ring3}, and A_{Ring11}: (a) Case-1, (b) Case-2, (c) Case-3, and (d) Case-4

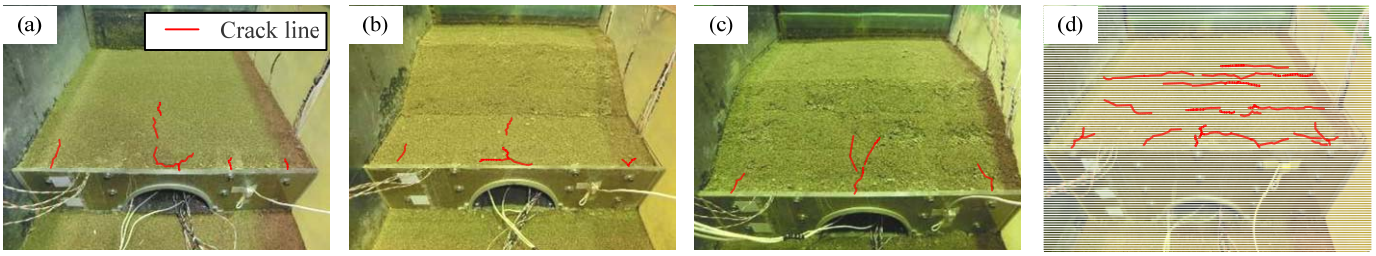

Figure 12. Embankment surface after experiment: (a) Case-1, (b) Case-2, (c) Case-3, and (d) Case-4

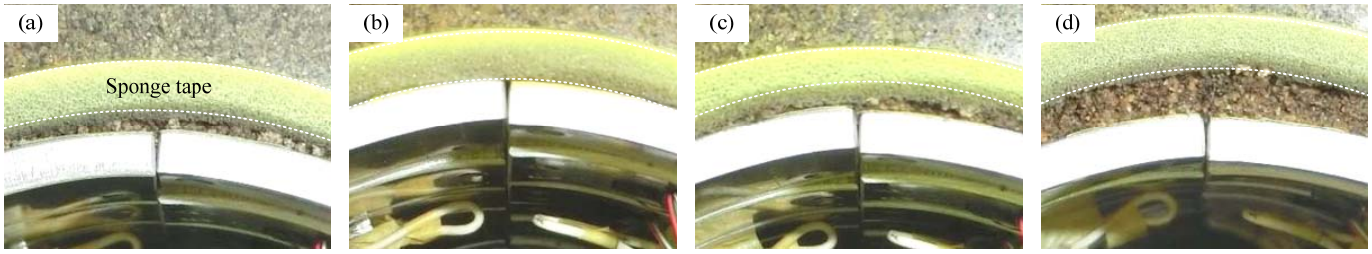

Figure 13. Crown hinge after experiment: (a) Case-1, (b) Case-2, (c) Case-3, and (d) Case-4